

# Orientation Control of $\text{Bi}_4\text{Ti}_3\text{O}_{12}$ Thin Film by Two-Dimensional RF Magnetron Sputtering

Tohru Higuchi, Mayumi Iwasa, Kazuhide Kudoh and Takeyo Tsukamoto

Department of Applied Physics, Tokyo University of Science, 1-3 Kagurazaka, Shinjuku, Tokyo 162-8601, Japan

Fax: 81-3-3260-4772, e-mail: higuchi@rs.kagu.tus.ac.jp

## ABSTRACT

The orientation control of ferroelectric  $\text{Bi}_4\text{Ti}_3\text{O}_{12}$  (BIT) thin film has been confirmed by two-dimensional RF magnetron sputtering with  $\text{Bi}_2\text{O}_3$  and  $\text{TiO}_2$  targets. When the RF powers of  $\text{Bi}_2\text{O}_3$  and  $\text{TiO}_2$  targets were fixed at 100 W and 200 W, respectively, the BIT thin film exhibited a chemical stoichiometric composition. The orientation of BIT thin film depends on thickness of  $\text{TiO}_2$  target. The BIT thin films prepared at  $\text{TiO}_2$  targets with thicknesses of 2.65 and 3.20 mm exhibited highly *c*-axis orientation and (117) orientation, respectively. These findings considered to be due to difference of sputtering rate with thicknesses of  $\text{TiO}_2$  targets.

Key words:  $\text{Bi}_4\text{Ti}_3\text{O}_{12}$  (BIT), two-dimensional RF magnetron sputtering, thin film, orientation control, targets thickness

## 1. INTRODUCTION

Ferroelectric thin films are widely focused on an application for nonvolatile ferroelectric random access memories (NV-FeRAM). In particular,  $\text{Bi}_4\text{Ti}_3\text{O}_{12}$  (BIT) are useful lead-free and fatigue-free ferroelectric material exhibiting superior ferroelectricity even when using Pt electrode. The BIT has an orthorhombic structure with lattice constants  $a=0.5459$ ,  $b=0.5410$ , and  $c=3.2815$  nm [1-3]. Its ferroelectric properties of spontaneous polarization ( $P_r$ ) and coercive field ( $E_c$ ) are anisotropic, i.e.,  $P_r=4$   $\mu\text{C}/\text{cm}^2$  and  $E_c=3.5$  kV/cm along the *c*-axis and  $P_r=50$   $\mu\text{C}/\text{cm}^2$  and  $E_c=40$  kV/cm perpendicular to the *c*-axis. The large  $P_r$  of *a*-axis takes advantage of reducing the memory cell area of a NV-FeRAM.

In recent years, deposition of BIT thin films has been extensively studied by several deposition techniques such as metalorganic decomposition (MOD) [4-6], and metalorganic chemical vapor deposition (MOCVD) [7-14] and RF magnetron sputtering methods [15-20]. From the point of view of commercial production using MOD and MOCVD methods, there are still some severe difficulties, for instance poor throughput (low deposition rate), high-temperature deposition, and poor reproducibility. In order to investigate the ferroelectric properties of BIT thin films, it is necessary to perform a more systematic optimization of deposition condition.

In this study, the BIT thin films were deposited on Pt/Ti/SiO<sub>2</sub>/Si substrates by two-dimensional RF magnetron sputtering method with  $\text{TiO}_2$  and  $\text{Bi}_2\text{O}_3$  ceramic multitargets. We tried to deposit BIT thin films by controlling RF powers of  $\text{Bi}_2\text{O}_3$  and  $\text{TiO}_2$  targets in order to control the compositions of Bi and Ti. Furthermore, the orientation control of BIT thin film was proved by changing the thickness of  $\text{TiO}_2$  target.

## 2. EXPERIMENTAL

BIT thin films were deposited by RF magnetron reactive sputtering using  $\text{TiO}_2$  and  $\text{Bi}_2\text{O}_3$  ceramic

multitargets. The  $\text{TiO}_2$  and  $\text{Bi}_2\text{O}_3$  ceramic targets were prepared as follows [17,18]. The  $\text{TiO}_2$  (Furuuchi chemical Co., Ltd., 99.99 %) powder was calcined at 1100°C for 2 hours, and pressed into disk (5 inch in diameter). The pressed  $\text{TiO}_2$  disk was sintered at 1250°C for 12 hours. The thickness of  $\text{TiO}_2$  target was changed from 2.65 to 3.20 mm. The  $\text{Bi}_2\text{O}_3$  (Furuuchi chemical Co., Ltd., 99.9 %) powder was calcined at 700°C for 2 hours, and pressed into disk (5 inch in diameter). The pressed  $\text{Bi}_2\text{O}_3$  disk was sintered at 750°C for 12 hours. The thickness of  $\text{TiO}_2$  target was fixed at 4.55 mm. These ceramic targets were examined using X-ray diffraction and scanning-electron-microscopy (SEM), as shown in Figs. 1 and 2. The density of  $\text{Bi}_2\text{O}_3$  and  $\text{TiO}_2$  targets were approximately 94 % and 98 %.

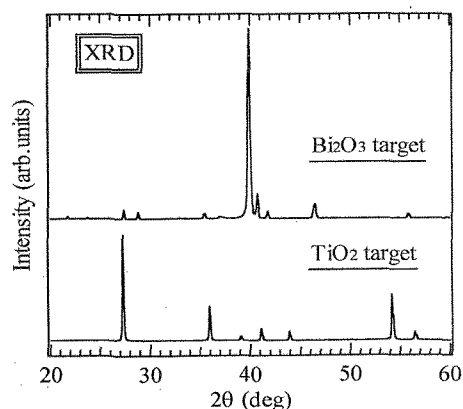


Fig. 1 XRD patterns of  $\text{Bi}_2\text{O}_3$  and  $\text{TiO}_2$  targets.

The deposition system was arranged in a symmetric configuration with a rotating substrate holder for compositional uniformity. The base pressure of the sputtering chamber was typically  $\sim 2 \times 10^{-8}$  Torr, and

substrates were inserted from a load lock into the main chamber to maintain a low base pressure. For the deposition of BIT thin films, an operating pressure of 10 mTorr was maintained during deposition. The total flow rates of Ar and  $\text{O}_2$  gases was 10 sccm, as controlled by mass-flow controllers, for the stoichiometric thin films. The distance from the target to the substrate was 8 cm in both  $\text{Bi}_2\text{O}_3$  and  $\text{TiO}_2$  targets. The substrate temperature was fixed at about  $600^\circ\text{C}$ . The deposition time was usually 60 min. As-deposited thin films were annealed in an oxygen flow.

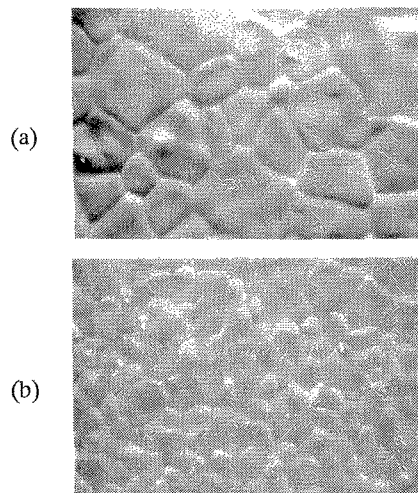


Fig.2 AFM images of (a)  $\text{Bi}_2\text{O}_3$  and (b)  $\text{TiO}_2$  targets.

The structural properties of the BIT thin films were characterized by X-ray diffraction (XRD) using  $\text{CuK}\alpha$ . Surface morphology was observed by SEM. Electrical properties were measured using the ferroelectric property measurement system RT-6000HVS manufactured by Radiant Technologies Inc. The polarization-electric field ( $P$ - $E$ ) hysteresis loops were measured using one-shot triangular waveforms with a period of 50 ms. The dielectric constant ( $\epsilon$ ) was measured with LCR meter.

### 3. RESULTS AND DISCUSSION

Figure 3 shows the input RF power dependence of the composition ratio of as-deposited BIT thin films on Pt/Ti/SiO<sub>2</sub>/Si substrates. The thicknesses of  $\text{TiO}_2$  and  $\text{Bi}_2\text{O}_3$  targets were fixed at 2.90 and 4.55 mm, respectively. We have already reported that the deposition rate of  $\text{Bi}_2\text{O}_3$  is higher than that of  $\text{TiO}_2$ . Therefore, the RF power was fixed at 200 W for the  $\text{TiO}_2$  target and was changed from 50 to 200 W for the  $\text{Bi}_2\text{O}_3$  target. Two dashed lines indicate the stoichiometric chemical composition of Bi (57.14 at.%) and Ti (42.86 at.%). The composition ratio depends on the input RF power applied to  $\text{Bi}_2\text{O}_3$ . When the RF power is 50 W, the composition ratios of Bi and Ti markedly differ from the chemical stoichiometric composition, indicating that the deposition rate of  $\text{Bi}_2\text{O}_3$  is significantly slower than that of  $\text{TiO}_2$ . The stoichiometric composition of the BIT thin film is obtained when the RF power applied to  $\text{Bi}_2\text{O}_3$  is 100 W.

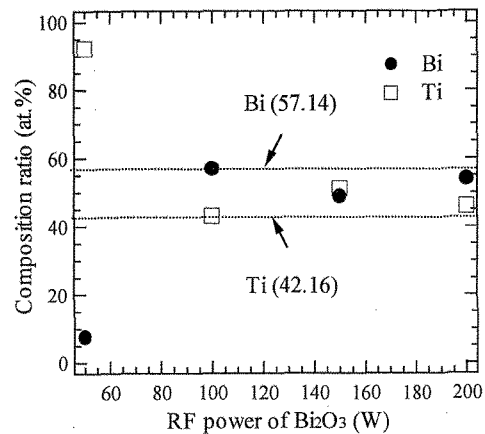


Fig. 3 Composition ratio as a function of RF power applied to the  $\text{Bi}_2\text{O}_3$  targets in as-deposited BIT thin films. The RF power applied to the  $\text{TiO}_2$  target is fixed at 200 W.

Figure 4 shows the XRD patterns of the BIT thin films under the conditions of Fig. 1. Pt peaks are shown at  $2\theta=41.0^\circ$  and  $46.5^\circ$ , which are designated as (111) and (200), respectively. Closed circles indicate the pyrochlore phase of  $\text{Bi}_2\text{Ti}_2\text{O}_7$ . The existence of pyrochlore phase is observed at 50, 150 and 200 W. The number of the pyrochlore phase is in proportion to the RF power, indicating that the deposition rate of Bi strongly depends on the RF power. The XRD pattern of 100 W shown as a solid line obviously exhibits a highly  $c$ -axis oriented BIT single phase, though the (117) peak is strongly observed.

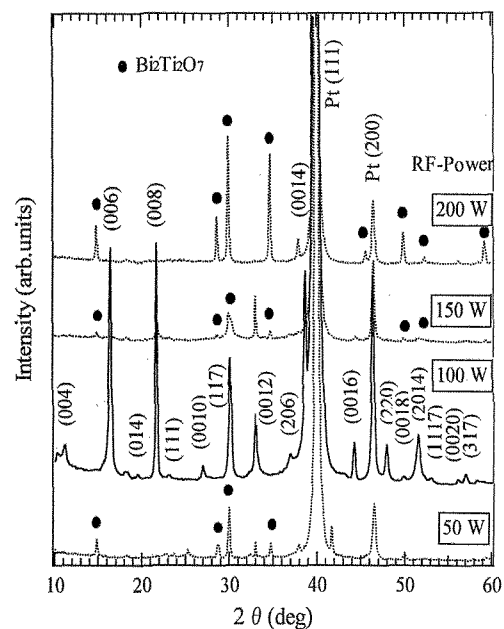


Fig. 4 XRD patterns of BIT thin films as a function of RF power applied to the  $\text{Bi}_2\text{O}_3$  targets in as-deposited BIT thin films. The RF power applied to the  $\text{TiO}_2$  target is fixed at 200 W. The closed circle indicates the existence of pyrochlore phase.

Figure 5 shows the composition ratio of as-deposited BIT thin film as a function of thickness of TiO<sub>2</sub> target. Closed circle and triangle marks indicate the composition of Bi and Ti, respectively. The thickness of Bi<sub>2</sub>O<sub>3</sub> target is fixed at 4.55 mm. In the TiO<sub>2</sub> target with thickness of 2.65 mm, the compositions of the BIT thin film are Bi-poor and Ti-rich. In the TiO<sub>2</sub> targets with thickness of 2.90 and 3.20 mm, the prepared BIT thin films exhibit chemical stoichiometric compositions. These results indicate that the sputtering rate of TiO<sub>2</sub> depends on the target thickness.

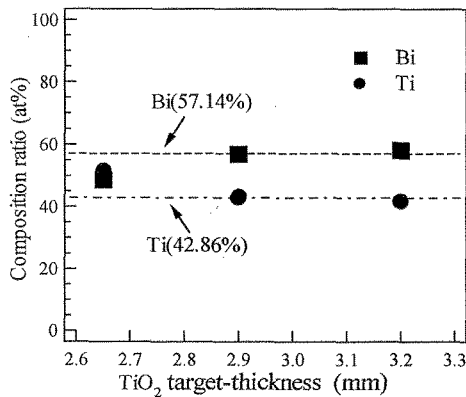


Fig. 5 Composition ratio as a function of thickness of TiO<sub>2</sub> target in as-deposited BIT thin films. The thickness of Bi<sub>2</sub>O<sub>3</sub> target is fixed at 4.55 mm.

Figure 6 shows the XRD patterns of the BIT thin films under the conditions of Fig. 5. Solid and broken lines indicate the post-annealed and as-deposited BIT thin films, respectively. In the TiO<sub>2</sub> targets with thickness of 2.90 mm, the as-deposited BIT thin film exhibits the existence of pyrochlore phase. The post-annealed BIT thin film exhibits highly *c*-axis orientation, though the (117) peak is also observed. In the TiO<sub>2</sub> targets with thickness of 3.20 mm, the as-deposited and post-annealed BIT thin films exhibit highly (117) oriented BIT single phase.

Figure 7 shows the hysteresis loops of post-annealed BIT thin films prepared at the TiO<sub>2</sub> targets with thicknesses of 2.65 and 3.20 mm. In as-deposited BIT thin films, the hysteresis loops were not observed. The *P-E* hysteresis loops are observed in both post-annealed films, though the loops do not saturate. The *P<sub>r</sub>* of post-annealed BIT thin films prepared at TiO<sub>2</sub> targets with thickness of 2.90 and 3.20 mm were  $2P_r = 3.0$  and  $24.3 \mu\text{C}/\text{cm}^2$ , respectively. The  $\epsilon$  at TiO<sub>2</sub> targets with thickness of 2.90 and 3.20 mm were 84 and 180, respectively. The  $\epsilon$  values are in good agreement with BIT single crystal. These values are superior to those of the BIT thin films deposited by one-dimensional RF magnetron sputtering with a stoichiometric BIT single target [15,16]. The small *P<sub>r</sub>* and small  $\epsilon$  at TiO<sub>2</sub> targets with thickness of 2.90 mm contributes highly *c*-axis orientation. The large *P<sub>r</sub>* and  $\epsilon$  at 3.20 mm TiO<sub>2</sub> targets with thickness contributes highly (117) orientation. The *E<sub>c</sub>* at TiO<sub>2</sub> targets with thickness of 2.90 and 3.20 mm were  $2E_c = 140$  and  $246 \text{ kV}/\text{cm}$ , respectively. The large *E<sub>c</sub>* in both films are considered to be large leakage current ( $\sim 10^{-6} \text{ A}/\text{cm}$ ).

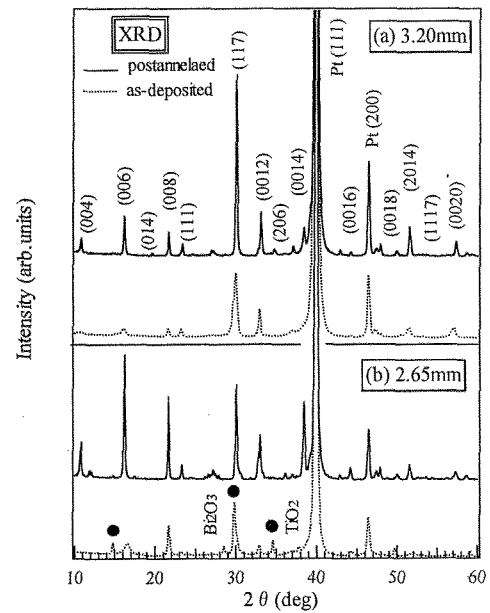


Fig. 6 Comparison of XRD patterns between as-deposited and post-annealed BIT thin films. The thickness of TiO<sub>2</sub> target is 2.65 and 3.20 mm. The thickness of Bi<sub>2</sub>O<sub>3</sub> target is fixed at 4.55 mm.

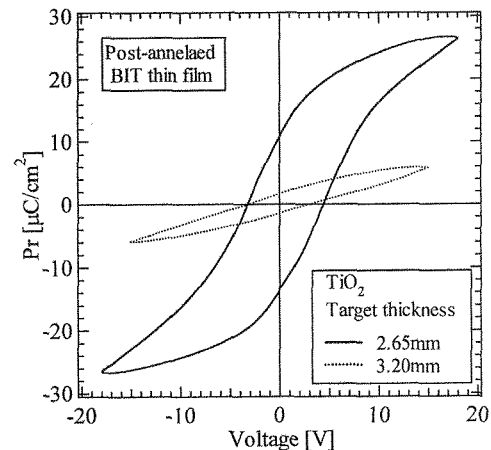


Fig. 7 Comparison of *P-E* hysteresis loop as a function of thickness of TiO<sub>2</sub> target in post-annealed BIT thin films.

Figure 8 shows (a) an AFM image and (b) a SEM cross-sectional micrograph of the post-annealed BIT thin film prepared at the TiO<sub>2</sub> targets with thickness of 3.20 mm. The BIT thin film consisted of well-developed grains with diameters of around 400 nm. The grain shape was isotropic and round. It was also observed from the SEM micrograph that one or two grains were stacked along the out-of-plane direction. The large *E<sub>c</sub>* shown in Fig. 7 attributes the large grain size. The contribution of oxygen vacancies might also exist in the film.

The above results indicate that the orientation control of BIT thin film is possible by changing the thickness of TiO<sub>2</sub> targets with low sputtering rate, though the reason has not been clarified in this study.

To further investigate the electrical and structural properties of the BIT thin films on Pt substrates, we must perform a more systematic optimizations of the deposition condition.

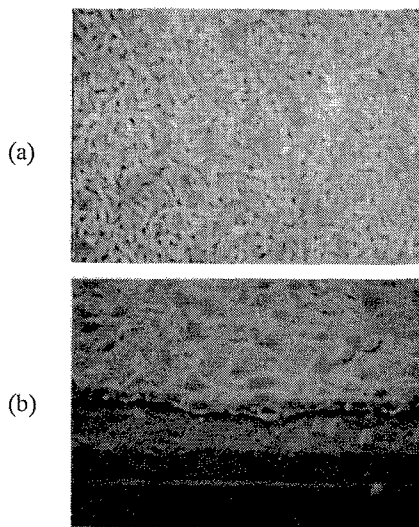


Fig. 8 (a) AFM image and (b) SEM cross-sectional micrograph of post-annealed BIT thin film prepared at the  $\text{TiO}_2$  target with the thickness of 3.20 mm.

#### 4. CONCLUSION

We have proposed novel process for the fabrication of BIT thin films by the two-dimensional RF magnetron sputtering method with  $\text{TiO}_2$  and  $\text{Bi}_2\text{O}_3$  targets. The composition ratio of BIT thin films depends on the RF power applied to  $\text{Bi}_2\text{O}_3$ . When the RF powers of  $\text{Bi}_2\text{O}_3$  and  $\text{TiO}_2$  targets were fixed at 100 W and 200 W, respectively, the prepared BIT thin films exhibited stoichiometric composition. Furthermore, the orientation of BIT thin film depends on thickness of  $\text{TiO}_2$  target. The BIT thin films prepared at  $\text{TiO}_2$  targets with thicknesses of 2.65 and 3.20 mm exhibited highly *c*-axis orientation and (117) orientation, respectively. The  $P_r$  of the BIT thin films prepared at  $\text{TiO}_2$  targets with thickness of 2.90 and 3.20 mm were  $2P_r = 3.0$  and  $24.3 \mu\text{C}/\text{cm}^2$ , respectively, when the thicknesses of  $\text{Bi}_2\text{O}_3$  target is fixed at 4.55 mm.

#### ACKNOWLEDGEMENTS

We would like to thank Mr. M. Tanaka for his useful discussion. This work was partially supported by the Foundation for Materials Science and Technology of Japan (MST Foundation), and the Grant-In-Aid for Scientific Research from the Ministry of Education, Cultures, Sports, Science and Technology.

#### REFERENCES

- [1] E. C. Subbarao: Phys. Rev. **122** (1961) 804.
- [2] S. E. Cummins and L. E. Cross: Appl. Phys. Lett. **10** (1967) 14.
- [3] R. W. Wolfe and R. E. Newnham: J. Electrochem. Soc. **116** (1967) 832.
- [4] A. Kakimi, S. Okamura and T. Tsukamoto: Jpn. J. Appl. Phys. **33** (1994) L 1707.
- [5] S. Okamura, Y. Yagi, K. Mori, G. Fujihashi, S. Ando and T. Tsukamoto: Jpn. J. Appl. Phys. **36** (1997) 5889.
- [6] M. Yamaguchi and T. Nagatomo: Thin Solid Films **348** (1999) 294.
- [7] R. Muhammet, T. Nakamura, M. Shimizu and T. Shiosaki: Jpn. J. Appl. Phys. **33** (1994) 5215.
- [8] T. Tsukamoto and S. Okamura: Ferroelectrics **170** (1995) 77.
- [9] T. Kijima and H. Matsunaga: Jpn. J. Appl. Phys. **37** (1998) 5171.
- [10] T. Watanabe and H. Funakubo: Jpn. J. Appl. Phys. **39** (2000) 5211.
- [11] T. Watanabe, A. Saiki, K. Saito and H. Funakubo: J. Appl. Phys. **89** (2001) 3934.
- [12] T. Watanabe, H. Funakubo, M. Osada, Y. Noguchi and M. Miyayama: Appl. Phys. Lett. **80** (2002) 100.
- [13] M. Nakamura, T. Higuchi and T. Tsukamoto: Jpn. J. Appl. Phys. **42** (2003) 5687.
- [14] M. Nakamura, T. Higuchi and T. Tsukamoto: Jpn. J. Appl. Phys. **42** (2003) 5969.
- [15] Y. Masuda, H. Masumoto, A. Baba, T. Goto and T. Hirai: Jpn. J. Appl. Phys. **32** (1993) 4043.
- [16] W. Jo, S. M. Cho, H. M. Lee, D. C. Kim and J. U. Bu: Jpn. J. Appl. Phys. **38** (1999) 2827.
- [17] M. Tanaka, T. Higuchi, K. Kudoh and T. Tsukamoto: Jpn. J. Appl. Phys. **41** (2002) 1536.
- [18] K. Kudoh, T. Higuchi, Y. Iwasa, M. Hosomizu and T. Tsukamoto: Proc. Inter. Symp. Appl. Ferro. (ISAF) **XIII** (2002) 167.
- [19] T. Higuchi, M. Tanaka, K. Kudoh, T. Takeuchi, S. Shin and T. Tsukamoto: Jpn. J. Appl. Phys. **40** (2001) 5803.
- [20] T. Higuchi, K. Kudoh, T. Takeuchi, Y. Masuda, Y. Harada, S. Shin and T. Tsukamoto: Jpn. J. Appl. Phys. **41** (2002) 7195.

(Received October 11, 2003; Accepted March 10, 2004)